Regular Article

IMMUNOBIOLOGY

Autoimmunity, hypogammaglobulinemia, lymphoproliferation, and mycobacterial disease in patients with activating mutations in *STAT3*

Emma M. Haapaniemi,[1] Meri Kaustio,[2] Hanna L. M. Rajala,[3] Arjan J. van Adrichem,[2] Leena Kainulainen,[4] Virpi Glumoff,[5] Rainer Doffinger,[6] Heikki Kuusanmäki,[2] Tarja Heiskanen-Kosma,[7] Luca Trotta,[2] Samuel Chiang,[8] Petri Kulmala,[5,9] Samuli Eldfors,[2] Riku Katainen,[10] Sanna Siitonen,[11] Marja-Liisa Karjalainen-Lindsberg,[11] Panu E. Kovanen,[12] Timo Otonkoski,[13,14] Kimmo Porkka,[3] Kaarina Heiskanen,[15] Arno Hänninen,[16] Yenan T. Bryceson,[8] Raija Uusitalo-Seppälä,[17] Janna Saarela,[2] Mikko Seppänen,[18] Satu Mustjoki,[3] and Juha Kere[1,19]

[1]Folkhälsan Institute of Genetics and Research Programs Unit, Molecular Neurology, and [2]Institute for Molecular Medicine Finland, University of Helsinki, Helsinki, Finland; [3]Hematology Research Unit Helsinki, Department of Hematology, University of Helsinki and Helsinki University Central Hospital Cancer Center, Helsinki, Finland; [4]Department of Pediatrics and Department of Medicine, Turku University Hospital, Turku, Finland; [5]Department of Medical Microbiology and Immunology, Medical Research Center Oulu, Oulu University Hospital and University of Oulu, Oulu, Finland; [6]Department of Clinical Biochemistry and Immunology, Addenbrooke's Hospital and National Institute for Health Research, Cambridge Biomedical Research Center, Cambridge, United Kingdom; [7]Department of Pediatrics, Kuopio University Hospital, Kuopio, Finland; [8]Center for Infectious Medicine, Department of Medicine, Karolinska Institutet, Stockholm, Sweden; [9]Department of Pediatrics, Medical Research Center Oulu, Oulu University Hospital and University of Oulu, Oulu, Finland; [10]Department of Medical Genetics, Genome-Scale Biology Research Program, Institute of Biomedicine, University of Helsinki, Helsinki, Finland; [11]Laboratory Services (Hospital District of Helsinki and Uusimaa Laboratory), [12]Department of Pathology, and [13]Children's Hospital, Helsinki University Central Hospital, Helsinki, Finland; [14]Research Programs Unit, Molecular Neurology, University of Helsinki, Helsinki, Finland; [15]Children's Hospital, Helsinki University Central Hospital, Helsinki, Finland, [16]Department of Medical Microbiology and Immunology, University of Turku, Turku, Finland; [17]Department of Infectious Diseases, Satakunta Central Hospital, Pori, Finland; [18]Immunodeficiency Unit, Department of Medicine, Helsinki University Central Hospital, Helsinki, Finland; and [19]Department of Biosciences and Nutrition, and Center for Innovative Medicine, Karolinska Institutet, Stockholm, Sweden

Key Points

- Germline activating STAT3 mutations were detected in 3 patients with autoimmunity, hypogammaglobulinemia, and mycobacterial disease.

- T-cell lymphoproliferation, deficiency of regulatory and helper 17 T cells, natural killer cells, dendritic cells, and eosinophils were common.

The signal transducer and activator of transcription (STAT) family of transcription factors orchestrate hematopoietic cell differentiation. Recently, mutations in *STAT1*, *STAT5B*, and *STAT3* have been linked to development of immunodysregulation polyendocrinopathy enteropathy X-linked–like syndrome. Here, we immunologically characterized 3 patients with de novo activating mutations in the DNA binding or dimerization domains of *STAT3* (p.K392R, p.M394T, and p.K658N, respectively). The patients displayed multiorgan autoimmunity, lymphoproliferation, and delayed-onset mycobacterial disease. Immunologically, we noted hypogammaglobulinemia with terminal B-cell maturation arrest, dendritic cell deficiency, peripheral eosinopenia, increased double-negative (CD4⁻CD8⁻) T cells, and decreased natural killer, T helper 17, and regulatory T-cell numbers. Notably, the patient harboring the K392R mutation developed T-cell large granular lymphocytic leukemia at age 14 years. Our results broaden the spectrum of phenotypes caused by activating *STAT3* mutations, highlight the role of STAT3 in the development and differentiation of multiple immune cell lineages, and strengthen the link between the STAT family of transcription factors and autoimmunity. (*Blood*. 2015;125(4):639-648)

Introduction

Primary immunodeficiency syndromes are a heterogeneous group of diseases with variable manifestations, including autoimmunity. The most characteristic early-onset autoimmunity syndrome is immuno-dysregulation polyendocrinopathy enteropathy X-linked (IPEX) syndrome, which leads to fatal autoimmunity unless treated with stem cell transplantation. IPEX is associated with recessive mutations in *FOXP3,* encoding a transcription factor essential for regulatory T-cell

(Treg) development.[1] Other genetic causes include mutations in *CD25*, *STAT1*, *STAT5B*, and *ITCH*.[2-4]

The signal transducer and activator of transcription (STAT) transcription factors are widely expressed in hematological and other cell types, and mutations causing either gain or loss of STAT activity have been associated with primary immunodeficiency syndromes.[2,5-8] The cytokine receptor–Janus kinase–STAT pathway has an important role

in the regulation of the immune system, and different STAT family members have been ascribed specific roles in determining T-cell differentiation in response to certain cytokines. Generally, T helper 1 (Th1) cell differentiation is mediated by the interferon-γ (IFN-γ)–STAT1 and interleukin-12 (IL-12)–STAT4 axis, Th2 differentiation by the IL-4–STAT6 axis, Th17 by the IL-6–STAT3 axis, and commitment to Treg pathway by the IL-2–STAT5 axis.[9,10] Consequently, mutations in *STAT* genes lead to variable clinical presentations, ranging from susceptibility to viral infections and mycobacterial disease to multiorgan autoimmunity.[2,5-8] As an example, dominant-negative germline mutations in *STAT3* cause hyperimmunoglobulin E (IgE) syndrome (HIES),[5,6] whereas recently discovered somatic activating *STAT3* mutations have been found in 40% to 70% cases of large granular lymphocytic (LGL) leukemia, a neoplastic disease accompanied by autoimmune manifestations such as rheumatoid arthritis and autoimmune cytopenias.[11-13]

We evaluated 3 patients who carried germline heterozygous activating *STAT3* mutations, 2 of which were recently published as part of a larger cohort featuring 5 STAT3 gain-of-function patients.[14] The 2 patients presented with aggressive multiorgan autoimmunity and lymphoproliferation, including pediatric LGL leukemia. The third patient first described here had late-onset autoimmune manifestations and developed disseminated mycobacterial disease in late adolescence. Immunologically, we noted hypogammaglobulinemia with terminal B-cell maturation arrest, dendritic cell deficiency, peripheral eosinopenia, increased double-negative (CD4⁻CD8⁻) T cells, and low natural killer (NK), Th17, and regulatory T-cell counts.

Methods

Study patients

We evaluated 2 patients characterized by early-onset autoimmunity and growth failure previously published as part of a larger autoimmunity cohort[14] and 1 with delayed-onset disseminated nontuberculous mycobacteriosis (Table 1; Figure 1; detailed case descriptions are in the supplemental Appendix on the *Blood* Web site). Patient 1 is a 17-year-old female born full term without complications. She was first brought to medical attention at 12 months of age for diarrhea and abdominal pain caused by autoimmune enteropathy. At the age of 2, she developed generalized, livedo-like exfoliating dermatitis (Figure 1). At age 6, marked and progressive lymphadenopathy and splenomegaly were noted, with lymph node biopsy showing polyclonal CD4⁺ T-cell expansion. At age 10, she suffered from sicca and was diagnosed with bilateral posterior uveitis with cystic macular edema that has since led to severe visual impairment. She also experienced recurrent autoinflammatory episodes with high fever, sterile pleuritis, and serositis with concomitant rise in inflammatory markers. Her growth was retarded and alternated between −2 standard deviations (SD) to −4 SD. Because of recurrent upper respiratory tract infections since birth, multiple tympanostomies and functional endoscopic sinus surgery were performed at age 11. From early school age, the patient has suffered from reversible bronchoconstriction and, at age 12, high-resolution computed tomography showed moderate bronchiectasis. Immunoglobulin replacement therapy was then introduced to treat mild unspecific hypogammaglobulinemia with positive response in her rate of infections. Recently, the patient developed rapidly worsening cryptogenic organizing pneumonia requiring invasive ventilation and high-dose steroids. At the time of sampling, she was using systemic tacrolimus and corticosteroid medication and was on intravenous immunoglobulin replacement therapy.

Patient 2 is a 15-year-old female who was born small for gestational age at week 34 (1380 g/40.5 cm/30.5 cm, −5 SD). At birth, she was diagnosed with neonatal diabetes mellitus with extremely high insulin, glutamate decarboxylase, and islet cell autoantibodies.[15] The patient suffered from multiple early-onset allergies. Despite initial height catch-up, worsening idiopathic growth

failure with gradual deterioration to −7 SD was noted. At age 12 months, she was diagnosed with celiac disease. The pancreas was rudimentary in the abdominal magnetic resonance imaging scan. She developed desquamative interstitial pneumonitis in infancy that later progressed to pulmonary fibrosis. At school age, she suffered from recurrent pneumonias. Gradually worsening and severe unspecific hypogammaglobulinemia was noted, leading to immunoglobulin replacement therapy at age 12. At age 14, the patient developed megaloblastic anemia (mean corpuscular volume 101, hemoglobin 6.0 g/L) with clonal T-cell LGL proliferation and was subsequently diagnosed with T-cell LGL leukemia. Recently, she developed relapsing thrombosis of the right internal carotid artery and suspected vasculopathy. She is currently dependent on weekly red blood cell transfusions. At the time of sampling, she was using systemic tacrolimus, high-dose steroids, and mycophenolate mofetil and was on intravenous immunoglobulin replacement therapy.

Patient 3 is a 22-year-old female with normal growth and development. Reactions to vaccinations, including the bacillus Calmette–Guérin vaccination, were normal. In early childhood, she had several ear infections leading to tympanostomy and adenotomy. At the age of 17, the patient presented with prolonged diarrhea and abdominal pain caused by lymphocytic colitis, which was successfully treated with peroral budesonide and loperamide. She also experienced episodes of marked immune thrombocytopenia and has reported swelling and stiffness in her small joints. At 19, the patient developed persistent fever from *Mycobacterium avium* pneumonia and was also diagnosed with antibody deficiency. The patient received immunoglobulin replacement therapy and standard treatment of mycobacterial infection with good response. At age 21, the patient developed fistulating cervical lymphadenitis with concomitant mediastinal and axillar lymphadenopathy. *M. avium* was found in a lymph node biopsy, bone marrow (BM), and feces. The patient is currently being treated with a combination of clarithromycin, ethambutol, and levofloxacin as well as intravenous immunoglobulin. At the time of sampling, no immunomodulatory drugs were being used.

This study was conducted in accordance to the principles of the Helsinki Declaration and was approved by the Helsinki University Central Hospital Ethics Committee. Written informed consent was obtained from all patients and healthy controls.

DNA and RNA extraction and selection of γδ T cells

Genomic DNA was extracted from freshly sorted T-cell fractions, EDTA blood samples, or salivary samples using the Qiagen FlexiGene DNA kit (Qiagen), Gentran puregene kit (Qiagen), or OraGene DNA Self-Collection Kit (OGR-250, DNA Genonek). RNA was extracted from heparin blood samples with the Qiagen miRNeasy kit (Qiagen). The CD3⁺γδ⁺ cell fraction (patient 2) was sorted from fresh peripheral blood mononuclear cells by flow cytometry using antibodies against CD3, CD8, CD3, T-cell receptor-αβ (TCR-αβ), and TCR-B-γδ (BD Biosciences).

Exome sequencing from whole blood, saliva, and γδ T-cell fractions and validation of candidate mutations

Whole exome sequencing was performed at the Institute for Molecular Medicine Finland sequencing core facility, Science for Life laboratory Stockholm, and University of Exeter according to established laboratory protocols. The read mapping, variant calling, and filtering steps for somatic and germline variants were performed as described previously.[12,16] The candidate mutations were verified by capillary sequencing from blood and salivary DNA samples. The primers are listed in supplemental Table 1.

STAT3 luciferase reporter assay and analysis of Y705-pSTAT3 in transiently transfected cells

The K658N, K392R, and M394T mutations were introduced into wild-type (WT) *STAT3* sequence in pDEST40 vector using the Phusion Site Directed Mutagenesis Kit (Thermo Scientific) (primer sequences are shown in supplemental Table 1). The STAT3 luciferase reporter assay and pSTAT3^Y705 western blotting were performed as previously described.[12] Briefly, HEK293 cells stably expressing a STAT3-responsive firefly luciferase reporter were

Table 1. Clinical manifestations of STAT3 gain-of-function patients

	Patient 1	Patient 2	Patient 3
STAT3 mutation	K658N	K392R	M394T
Sex	Female	Female	Female
Age (y)	17	15	22
Birthweight (SD)	0	−5	0
Growth (SD)	−4	−7	0
	Delayed puberty	Delayed puberty	Normal puberty
Infection susceptibility	Upper respiratory tract infections	Lower respiratory tract infections	Nontuberculous mycobacteria
	Severe dental caries	Severe dental caries	Lower respiratory tract infections
	Severe varicella		
Endocrine	Subclinical hypothyreosis with TPO positivity	Neonatal diabetes with positive IAA/GADA/ICA autoantibodies	—
Gastrointestinal	Autoimmune enteropathy	Celiac disease Rudimentary pancreas	Lymphocytic colitis
Skin	Generalized, livedo-like exfoliating dermatitis	—	Mild atopic-like eczema
Pulmonary	Cryptogenic organizing pneumonia, asthma-like symptoms, bronchiectasis	Desquamative interstitial pneumonitis	Nontuberculous mycobacteria
Hematology	Lymphadenopathy consisting of polyclonal CD4$^+$ cells hepatosplenomegaly BM eosinophilia Autoimmune hemolytic anemia	T-cell LGL leukemia BM eosinophilia Autoimmune hemolytic anemia	Immune thrombocytopenia
Autoinflammation	Sterile pleuritis or serositis with high fever and elevated inflammatory markers	—	—
Other	Sicca syndrome and bilateral posterior uveitis with cystic macular edema	Severe allergy	—

IAA, insulin autoantibodies; GADA, glutamic acid decarboxylase autoantibodies; ICA, islet cell autoantibodies; TPO, antithyroid peroxidase antibody.

plated onto 96-well plates at 15 000 cells/well and, 6 hours after plating, transfected with empty, WT, or mutant STAT3 plasmids. The following day, the cells were starved for 3 hours and subsequently mock-treated or stimulated with IL-6 for 3 hours. The luciferase activity was measured with the One-Glo Luciferase Assay System (Promega) according to the manufacturer's recommendations. Equal plasmid transfection and STAT3 phosphorylation were assessed by western blotting using parallel-derived whole cell lysates. Mouse anti-STAT3 (9139, Cell Signaling Technology; 1:1000), polyclonal rabbit anti-human pSTAT3^{Y705} (9131, Cell Signaling Technology; 1:1000), and mouse anti–α-tubulin (T902, Sigma-Aldrich; 1:1000) were used as primary antibodies. Secondary antibodies were goat anti-rabbit IRDye 800 (Li-cor Odyssey 926-32211; 1:1:15.000) and goat anti-mouse IRDye 680 (Li-cor Odyssey 926-32220; 1:1:15.000). Statistical significance was calculated using 2-way analysis of variance.
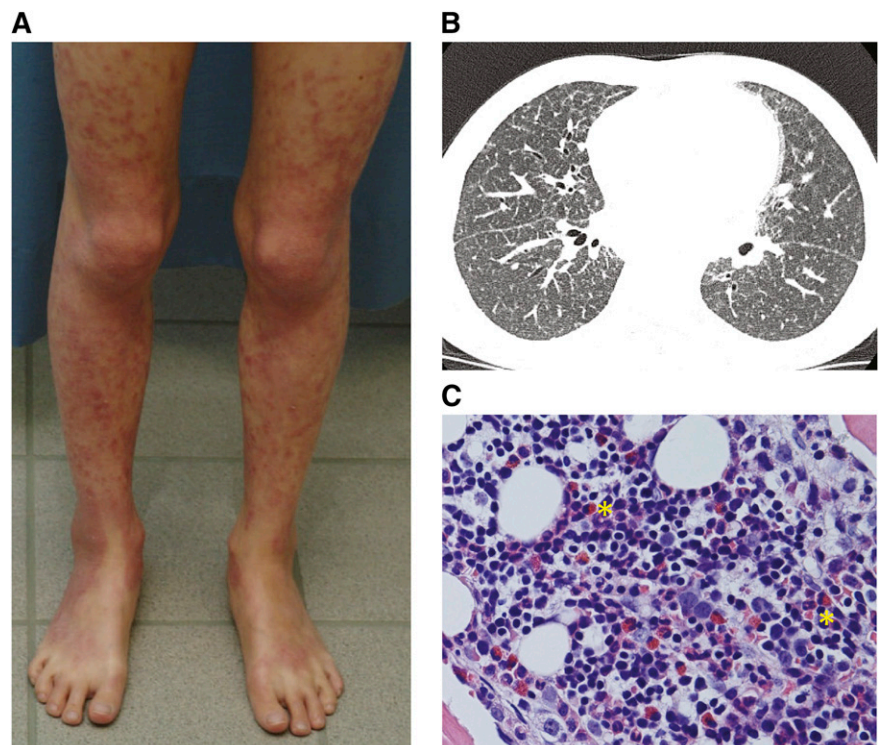
Figure 1. Clinical characteristics of patients. (A) Livedo-like generalized exfoliating dermatitis in patient 1. The rash culminates in limb extensor areas. (B) High-resolution computed tomography of patient 2 showing ground-glass opacity, bronchoalveolar thickening, and increased nodularity. (C) BM biopsy from patient 1 showing modest BM eosinophilia despite observed peripheral eosinopenia (yellow asterisks). Hematoxylin and eosin stain, original magnification ×40.
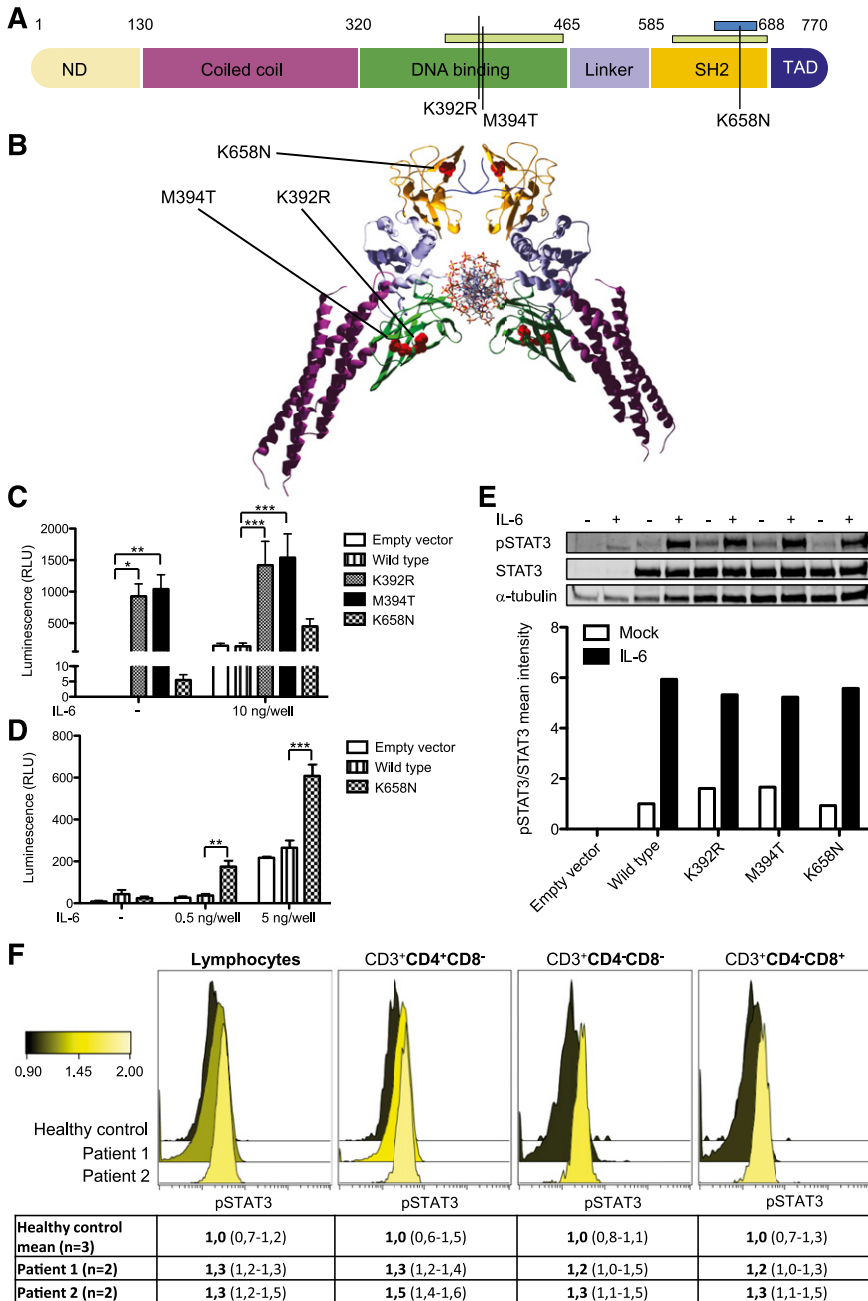
Figure 2. STAT3 mutations K658N, K392R, and M394T in studied patients. (A) Schematic representation of STAT3 protein domains with the observed mutations marked as black lines. Germ-line and somatic mutation hotspots for HIES[5,6] and LGL leukemia[11-13] are indicated as green and blue bars, respectively, at top. (B) Crystallographic structure of STAT3 dimer (RCSB Protein Data Bank code 1BG1). K658N, K392R, and M394T mutations are indicated as red dots. (C-D) HEK293 cells containing STAT3-responsive luciferase were transfected with empty, WT, and mutant STAT3 overexpression plasmids with or without IL-6 stimulation. K392R and M394T significantly increased STAT3 transcriptional activity in basal and stimulated conditions. Error bars represent standard error of the mean (n = 6; C). The K658N mutant showed hypersensitivity to IL-6 stimulation in low concentrations. Error bars represent standard error of the mean (n = 3; D). Two-way analysis of variance, $*P < .05$, $**P < .01$, and $***P < .001$. (E) No significant increase in pSTAT3^Y705 phosphorylation was observed when HEK293 cells were transfected with mutant STAT3-overexpression constructs. Equal amounts of parallel-derived whole cell lysates were loaded per condition. α-tubulin and STAT3 were used as loading and expression controls, respectively. +, presence of IL-6 stimulation; −, absence of IL-6 stimulation. (F) In peripheral blood, no significant increase in STAT3 phosphorylation was noted in studied patients. Color change indicates relative pSTAT3^Y705 expression. Forward panel, K392R; middle panel, K658N; back panel, healthy control (n = 3, value range presented in parentheses).

Immunophenotyping of T-, B-, and NK-cell subsets and peripheral blood Y705-pSTAT3 analysis

Fresh EDTA blood samples or peripheral blood mononuclear cell cultures (PBMNCs) were used for B- and T-lymphocyte immunophenotyping using a 4- or 6-color flow cytometry panel with monoclonal antibodies (mAbs) against the surface antigens IgM, IgD, CD3, CD4, CD8, CD16/56, CD19, CD21, CD27, CD33, CD34, CD38, CD45, CD56, CD57, CD133, HLA-DR, CD62L, CD45RA, CD45RO, and Ki-67 (BD Biosciences).[17] The memory status of T cells was studied with the antibody panel including anti-CD45 (clone 2D1), anti-CD3 (SK7), anti-CD4 (SK3), anti-CD45RA (GB11), and anti-CCR7 (150503) (R&D Systems).[17] Phosphorylated STAT3 (pSTAT3^Y705) expression was assessed using Y705-pSTAT3-PeCF594 (catalog no. 562673, BD Biosciences). For Treg analysis, anti–CD4-PerCP (BD345770), anti–CD25-APC (BD555434), and anti–CD127-PE (BD557938) mAbs (BD Biosciences) were used for surface staining and FOXP3 Alexa fluor 488 mAbs (320112, BioLegend) for intracellular staining (eBioscience).

For phenotyping of IL-17–positive Th17 cells, fresh PBMNCs were stimulated for 16 hours with anti-CD3/anti-CD28 beads (Life Technologies) in the presence of Brefeldin A (Sigma-Aldrich). Thereafter, the cells were fixed, permeabilized, and stained with anti-CD4 (Alexa Fluor 488 BD557695), CD69-APC (BD555533), and IL-17A-PE (BD560486) (BD Biosciences). Samples from patients 2 and 3 were additionally stained with CD161-APC-Cy7 (BD557756) (BD Biosciences). Samples were analyzed with FACSAria II or FACSCanto II flow cytometer and FACSDiva (BD Biosciences) or FlowJo software (TreeStar Inc).

Evaluation of Treg suppressor capacity and NK and CD3+CD8−–mediated cell cytotoxicity

CD4+CD25+CD127− Treg cells were sorted from whole blood using Human CD4+ T Cell Enrichment Cocktail (Stemcell Technologies) and fluorescence-activated cell sorting with mAbs against CD4-PerCP (BD345770), CD25-APC (BD555434), and CD127-PE (BD557938) (BD Biosciences). The cells
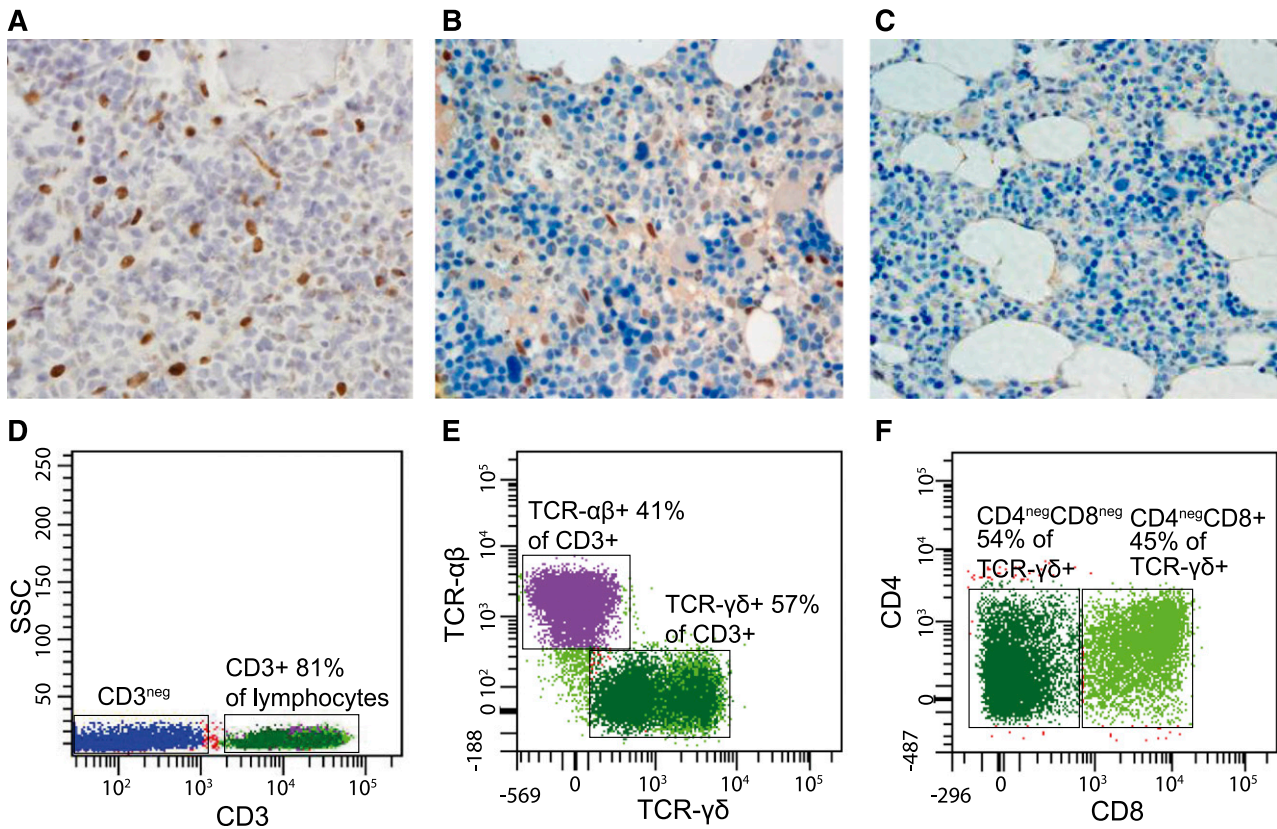
Figure 3. Abnormal lymphocyte populations detected in STAT3-mutated patients. (A-C) BM biopsy shows abnormally high number of phospho-STAT3–positive lymphocytes both in patient 2 (p.K392R) (A) and, to a lesser extent, in patient 1 (p.K658N) (B). Patient 3 (M394T) was not available for study. In healthy BM, no phospho-STAT3 cells are present (C). (D-F) Flow cytometry results from patient 2 (p. K392R). The majority of lymphocytes were $CD3^+$ (A), with 57% of the population expressing TCR-γδ (B). The TCR-γδ$^+$ population consisted of $CD4^-CD8^-$ and $CD4^-CD8^+$ T cells. The expression of TCR-γδ was considerably lower in $CD4^-CD8^-$ cells than in $CD4^-CD8^+$ T cells; therefore, 2 populations are seen in the scatter plot. (C). In healthy individuals, TCR-γδ–expressing T cells account less than 6% of all $CD3^+$ T cells and the TCR-γδ expression is normally uniform. ×40 magnification, hematoxylin and eosin stain.

were incubated for 6 days with carboxyfluorescein diacetate succinimidyl ester–labeled autologous responder T cells in ratios of 1:0.5, 1:1, and 1:2 for patient 1 and in a ratio of 1:2 for patients 2 and 3. Anti-CD3/anti-CD28 beads (Life Technologies) were used as stimulus. $CD4^+$ cells were analyzed using FACSAria II flow cytometer (BD Biosciences). The suppression percentage was calculated with the following formula: $100 - ([\% \text{ proliferation in presence of Treg}/\% \text{ proliferation in absence of Treg}] \times 100).$[18]

Evaluation of T- and NK-cell responses is described in detail elsewhere.[17,19] For the assessment of T-cell activation and degranulation, fresh mononuclear cells were stimulated for 6 hours with anti-CD3, anti-CD28, and anti-CD49d (BD Biosciences). For NK cell degranulation, cytokine and cytotoxicity assays, fresh mononuclear cells or fluorescence-activated cell–sorted $CD3^-CD16/56^+$ NK cells were stimulated with K562 target cells for 6 hours. The cells were analyzed using a 4- or 6-color flow cytometry panel with mAbs against the antigens CD45, CD3, CD4, CD8, CD16, CD56, CD45, CD45RA, TCR-γ, CCR7, IFN-γ, and tumor necrosis factor (TNF). Additionally, standard 4-hour chromium 51 (^{51}Cr)-release assays were performed according to established protocols for clinical samples using magnetic bead–separated $CD3^+CD8^+$ T-cell or $CD3^-CD56^+$ NK-cell subsets.[19,20]

Cytokine production

Whole blood was diluted 1:5 with RPMI into 96-well plates and activated by single stimulation or costimulations as indicated with IL-12 (20 ng/mL; R&D Systems; Abingdon), phytohemagglutinin (10 µg/mL; Sigma-Aldrich), lipopolysaccharide (LPS) (1 µg/mL; List Biochemicals), IFN-γ (2 × 10 exp IU/mL; Immukin, Boehringer Ingelheim), IL-18 (20 ng/mL; R&D Systems; Abingdon), bacillus Calmette–Guérin (SSI; 3.4 × 10 exp 4/well), phorbol 12-myristate 13-acetate (10 ng/mL, Sigma), and ionomycin (1 µg/mL; Sigma). Supernatants were taken at 24 hours. Cytokines were measured using

standard enzyme-linked immunosorbent assay according to the manufacturer's recommendations (IFN-γ; Pelikine, Sanquin, NL), or multiplexed particle-based flow cytometry (TNF-α, IL-12, IL-10, IL-6, IL-17; R+D Systems Fluorokinemap) on a Luminex analyzer (Bio-Plex, Bio-rad, UK).

For evaluation of IFN-γ signaling in monocytes, PBMNCs were plated in flat-bottomed 96-well plates (Costar Corning #3596) at 0.5×10^6 cells/well and stimulated with IFN-γ (0.01 ng/mL-150 ng/mL; Immunotools) for 60 minutes. PBMNCs were thereafter fixed, permeabilized, and stained with fluorescein isothiocyanate–anti-CD14 (11-0149) and phycoerythrin–anti-pSTAT1 (12-9008) antibodies according to manufacturer's protocol (eBioScience). STAT1 phosphorylation was determined in $CD14^+$ monocytes using flow cytometry. To assess Toll-like receptor signaling in monocytes, PBMNCs were stimulated with 100 ng/mL LPS (Sigma Aldrich) or left unstimulated for 60 minutes. L-selectin shedding was determined from $CD14^+$ monocytes by flow cytometry with antibodies against anti-phycoerythrin–anti-CD62L (12-9008) and fluorescein isothiocyanate–anti-CD14 (11-0149). Flow cytometry was performed with Accuri cytometer and the manufacturer's software (Becton Dickinson).

Anti-cytokine serology was performed by multiplexed particle-based flow cytometry as previously described.[21] Serum IgG antibodies to the following cytokines were investigated: IFN-γ, TNF, IL-12, IL-23, IFN-α, IFN-ω, IL-6, IL-17A, IL-17F, IL-22, and granulocyte macrophage–colony-stimulating factor.

Immunohistochemical staining of phospho-STAT3 and cleaved caspase-3

Immunohistochemistry (IHC) of BM biopsy paraffin sections was performed according to standard techniques using pSTAT3^{Y705} mAb (1:100; 9145S, Cell

Table 2. Immunologic features of patients with STAT3 gain-of-function mutations

		Normal range/healthy control median value	Patient 1 (K658N)	Patient 2 (K392R)	Patient 3 (M394T)
Leukocytes		3400-8200	7100	6900 (7500)*	5900
	Lymphocytes	1000-4500	1700	4278 (1270)*	820 ↓
	Monocytes	200-800	600	690 (370)*	570
	Neutrophils	1500-7500	4800	1750 (5830)*	4130
	Basophils	0-100	0	182 (0)*	80
	Eosinophils	100-400	0 ↓	10 (0)*↓	280
	Platelets	150 000-360 000	267 000	290 000 (266 000)*	271 000
	NK cells (CD3$^-$CD16$^+$/56$^+$)	90-600 (12%)	12 (0.7%) ↓	128 (3%) (38, 0.5%)* ↓	40-90 (4-13%) ↓
	NK cell function and maturation		Normal	Normal	Normal
Dendritic cells					
Plasmacytoid	lin$^-$HLA-DR$^+$CD123$^+$CD11c$^-$	0.1-0.3%	0.06% ↓	<0.01% ↓	0.01% ↓
Monocytoid	lin$^-$HLA-DR$^+$CD123$^-$CD11c$^+$	0.1-0.3%	0.2%	<0.01% ↓	0.73% ↑
CD3$^+$ T cells		**700-2100 (71%)**	**1462 (86%)**	**3507 (82%) (1092, 86%)***	**474 (74%)**
	TCRαβ$^+$	94%	94%	45% ↓ (93%)*	97%
	TCRγδ $^+$	6%	6%	55% ↑ (7%)*	3%
	CD57$^+$	21%	8.4%	65% ↑	65% ↑
	CD4$^-$CD8$^-$	4.2%	3.4%	30% (2.3%)* ↑	6%
	CD4$^-$CD8$^-$ TCRαβ$^+$	<3.4%	1.6%	1%	5% ↑
	CD4$^-$CD8$^-$ TCRγδ $+$	NA	1.8%	29%↑	1%
CD3$^+$CD4$^+$ T cells		**458-1406 (60%)**	**789 (54%)**	**666 (19%) ↓ (380, 34.8%)***	**307 (48%) ↓**
	CD45RO$^+$	51%	46%	70% ↑	NA
	CD45RA$^+$	47%	51%	26% ↓	18% ↓
	Ki-67$^+$	2%	2,50%	1.80%	NA
	HLA-DR$^+$	3%	29%	1.90%	NA
TCM	CCR7$^+$CD45RA$^-$	38%	44%	54% ↑	56% ↑
Naive	CCR7$^+$CD45RA$^+$	45%	50%	24% ↓	20% ↓
TEM	CCR7$^-$CD45RA$^-$	11%	5%	22% ↑	23% ↑
Temra	CCR7$^-$CD45RA$^+$	4%	1%	1%	2%
	Granzyme B$^+$	1%	0.2%	1.9%	NA
Unstimulated	IFN-γ/TNF-α secretion	0%	0.2%	0.1%	Normal§
Stimulated	IFN-γ/TNF-α secretion	5%	7.3%	21.5% ↑	Normal§
Treg	FOXP3$^+$CD25$^+$	2.3-7.8%	1.45% ↓	(0.67%)* ↓	4.9%
Treg suppressive capacity			Low	Low	Normal
Th17†	CD69$^+$IL17$^+$	0.47-1.59%	0.13% ↓	(0.35%)* ↓	0.22 ↓
CD3$^+$CD8$^+$ T cells		**200-1200 (51%)**	**570 (39%)**	**1790 (51%) (339, 31%)***	**134 (21%)**
	CD45RO$^+$	41%	20%	5% ↓	NA
	CD45RA$^+$	72%	76%	93% ↑	68%
	Ki-67$^+$	1%	2,70%	16% ↑	NA
	HLA-DR$^+$	3%	29%	56% ↑	NA
TCM	CCR7$^+$CD45RA$^-$	8%	11%	3%	13%
Naive	CCR7$^+$CD45RA$^+$	35%	62% ↑	8% ↓	45% ↑
TEM	CCR7$^-$CD45RA$^-$	27%	8% ↓	4% ↓	22%
Temra	CCR7$^-$CD45RA$^+$	33%	19%	86% ↑	21%
	Granzyme B$^+$	11%	14.9%	0.2%	NA
Unstimulated	IFN-γ/TNF-α secretion	0%	0.1%	0.1%	Normal§
Stimulated	IFN-γ/TNF-α secretion	7.20%	4.50%	4.30%	Normal§
CD19$^+$ B cells		**70-230 (12%)**	**660 (9.3%)**	**174 (14%)***	**80 (11%)**
Transitional	CD38^{hi}IgM^{hi}	0.6-3.5%	3.4%	(0%)* ↓	0.4% ↓
Naive	CD27$^-$IgD$^+$	NA	70% ↑	(68%)* ↑	94% ↑
Mature B cells	CD21$^+$	11-45%	84% ↑	(70%)* ↑	88 ↑
Memory	CD27$^+$	15-45%	23%	(26%)*	4% ↓
Marginal zone-like	CD27$^+$IgD$^+$IgM$^+$	7.2-30.8%	19.5% ↑	(24.9%)* ↑	2.9%
Switched memory	CD27$^+$IgD$^-$IgM$^-$	6.5-29.2%	0.5% ↓	(0.5%)* ↓	<0.1 ↓
Plasmablasts	CD38^{++}IgM$^-$	—	0.0%	(0.37%)*	0.5
Activated	CD38^{low}CD21^{low}	0.6-3.5%	12.1% ↑	(22.5%)* ↑	11.7 ↑

CD3$^+$ T-cell, CD4$^+$ cell, CD8$^+$ cell, and CD19$^+$ cell numbers are indicated as absolute counts and relative percentages of all lymphocytes (%). Healthy control values are indicated either as absolute count ranges or medians (%).

↑, high value; ↓, low value; IVIG, intravenous immunoglobulin therapy; NA, not applicable; TCM, central memory T cell; TEM, effector memory T cell; Temra, effector memory RA T cell; Treg, regulatory T cell.

*Tested before onset of lymphoproliferation at 12 y of age.

†Of all activated CD3$^+$CD4$^+$ cells.

‡For detailed specification, see supplemental data.

§Test method differs from that of other patients.

Table 2. (continued)

		Normal range/healthy control median value	Patient 1 (K658N)	Patient 2 (K392R)	Patient 3 (M394T)
Immunoglobulins (prior IVIG)					
	IgG	6.8-15.0 g/L	5.8 ↓	2.8 ↓	0.16 ↓
	IgA	0.52-4.02 g/L	1.67	0.21	1.7
	IgM	0.47-2.84 g/L	3.38	1.44	0.6
	IgE	0-110 IU/L	0.7	0.5	<2
Complement		Classical., alternative, and mannan-binding lectin pathway hemolytic activities	Normal	Normal	Normal
Lymphocyte proliferative responses to mitogens		Phytohemagglutinin, concanavalin A, pokeweed mitogen	Normal	Normal	Normal
Lymphocyte chemotaxis			NA	NA	Normal
Specific antibodies against vaccine antigens		Tetanus, diphtheria, pneumococcal polysaccharide	Protective	Protective	Tetanus unprotective, others NA
Autoantibodies‡			TPO positive	Negative	Negative

CD3^{+} T-cell, CD4^{+} cell, CD8^{+} cell, and CD19^{+} cell numbers are indicated as absolute counts and relative percentages of all lymphocytes (%). Healthy control values are indicated either as absolute count ranges or medians (%).

↑, high value; ↓, low value; IVIG, intravenous immunoglobulin therapy; NA, not applicable; TCM, central memory T cell; TEM, effector memory T cell; Temra, effector memory RA T cell; Treg, regulatory T cell.

*Tested before onset of lymphoproliferation at 12 y of age.

†Of all activated CD3^{+}CD4^{+} cells.

‡For detailed specification, see supplemental data.

§Test method differs from that of other patients.

Signaling Technology) and cleaved caspase-3 mAB (1:300; Cell Signaling Technology). BM biopsy slides from 3 healthy individuals were used as controls.

Results

Gain-of-function *STAT3* mutations are associated with multisystemic autoimmunity and mycobacterial disease

Patients 1 and 2 were recently shown to carry heterozygous, activating mutations in *STAT3*.[14] The mutations (p.K658N at chr17:40474427 C>G and p.K392R at chr17:40481630 T>C) localized to the *STAT3* Src-like homolog 2 and DNA-binding domains (Figure 2A-B). Exome sequencing was used to identify a novel de novo missense *STAT3* mutation at position chr17:40481624 A>G resulting in methionine-to-threonine substitution at position 394 (M394T) in the *STAT3* DNA-binding domain in patient 3. To compare the functional effect of these mutations, we transiently transfected the HEK293 cell line stably expressing luciferase under a STAT3-specific site promoter with constructs encoding WT or mutated STAT3. For K392R and M394T mutations, we observed STAT3 transcriptional activation under basal conditions, suggesting that these mutants are constitutively active (Figure 2C). In the K658N mutant, there was no transcriptional activity under basal conditions, but the mutant showed higher STAT3 transcriptional activation to low IL-6 concentrations than WT STAT3, the effect of saturating in higher concentrations (Figure 2D).

Effects of *STAT3* mutations on STAT3 phosphorylation status

The phosphorylation of tyrosine residue 705 (pY705) of STAT3 is essential for the dimerization and activation of WT STAT3.[22] To evaluate whether the observed STAT3 hyperactivity was dependent on increased STAT3 phosphorylation, we used parallel-derived whole cell lysates of the transiently transfected HEK293 cells to determine the level of pSTAT3^{Y705} protein by western blotting both at baseline and after IL-6 stimulation. Expression of mutant pSTAT3^{Y705} was similar to WT (Figure 2E). Additionally, we assessed the expression of pSTAT3^{Y705} from fresh whole blood samples by a fluorescence-activated cell sorted–based phosphoflow method (Figure 2F). The

proportion of pSTAT3^{Y705}-positive lymphocytes ranged between upper normal to slightly increased in the K392R- and K658N-mutated patients.

Additionally, BM biopsies from patients 1 (K658N) and 2 (K392R) were stained for pSTAT3^{Y705} IHC. In both cases, we observed increased number of pSTAT3^{Y705}-positive cells (Figure 3A-C). Morphologically, the pSTAT3^{Y705}-positive BM-infiltrating cells were classified as LGL. The number of pSTAT3^{Y705}-positive lymphocytes was higher in the patient 2 carrying the K392R mutation, which could be related to the recently made T-cell LGL leukemia diagnosis (Figure 3A-B).

STAT3 hyperactivity is associated with peripheral eosinopenia, hypogammaglobulinemia, and deficiency of Treg, NK, and dendritic cells

The effects of the *STAT3* mutations K392R, K658N, and M394T on the properties, phenotype, and functionality of hematopoietic cells were analyzed in detail using IHC and flow cytometry (Table 2; Figure 1C). In the myeloid lineage of patients 1 (K658N) and 2 (K392R), we observed marked peripheral eosinopenia with modest BM eosinophilia, suggesting an eosinophil mobilization defect. The BM biopsies from both patients were stained with cleaved caspase-3 antibody to detect increased eosinophil apoptosis, but the results were comparable to healthy controls (data not shown). We also noted plasmacytoid dendritic cell deficiency in all patients. The other cells of the myeloid lineage showed normal maturation in the BM and normal peripheral blood counts.

The results of the lymphoid lineage analysis are presented in Table 2. The patients had normal overall CD3^{+}CD4^{+} and CD3^{+}CD8^{+} T- and CD19^{+} B-cell counts but low relative CD3^{−}CD16^{+}CD56^{+} NK-cell counts. In the more detailed analyses of cytotoxic lymphocyte subsets, the frequencies of early differentiated CD56^{bright} and late differentiated CD57^{+} NK cells were normal. The patients' NK cells expressed normal levels of cytotoxic granule constituents perforin, granzyme A, and granzyme B (data not shown). Moreover, NK-cell and cytotoxic CD3^{+}CD8^{+}CD57^{+} T-cell degranulation and target cell killing were also within normal range, as was IFN-γ and TNF production in response to engagement of

Table 3. Somatic mutations in the LGL clone of patient 2

Gene	Chromosome	Position	Ref. base	Var. base	Amino acid change	Allele frequency (%)	Sift/PolyPhen prediction	Somatic P value*
LY9	1	160788035	T	C	I457T	17.27	Tolerated/benign	8.97×10^{-6}
RB1CC1	8	53570332	G	C	P686R	10.29	Tolerated/benign	.00097
FOXP4	6	41533673	G	A	A59T	14.04	Tolerated/benign	.003229
ICOSLG	21	45649510	A	G	L442P	14.04	Tolerated/benign	.005479

PolyPhen, polymorphism phenotyping; Ref, reference; Var, variant.
*Somatic P value for somatic/loss of heterozygosity events.

immunoreceptor tyrosine–based activation motif –coupled activating receptors (data not shown). NK-cell killing of K562 target cells was also assessed and found to be within normal range (data not shown).

Over time, all patients developed unspecific hypogammaglobulinemia or antibody deficiency (Table 2). In B-cell subset analyses, the relative numbers of activated CD19$^+$CD38^{low}CD21^{low} B cells and CD19$^+$CD21$^+$ mature B cells were increased. Additionally, a rise in marginal zone–like CD19$^+$CD27$^+$IgD$^+$IgM$^+$ B cells with a corresponding decrease in CD19$^+$CD27$^+$IgD$^-$IgM$^-$ switched memory B cells was observed. The patients were screened for autoantibodies against endocrine and exocrine organs as well as intracellular proteins (for a detailed account, see supplemental Table 2). Patient 1 had positive antithyroid peroxidase (TPO) antibodies without clinical thyroid disease. Patient 2 had high titer diabetes autoantibodies. All other autoantibody titers were negative.

In the T-cell compartment, we noticed a deficiency of CD4$^+$CD25$^+$FOXP3$^+$ Treg cells in the IPEX-like patients 1 and 2 (Table 2). Also, the suppressive capacity of Treg cells was reduced (supplemental Figure 2). In patient 3, Treg cell counts and suppressive capacity were comparable to the controls. Surprisingly, the proportions of IL-17 producing CD4$^+$CD69$^+$ Th17 cells were also decreased in all patients. To confirm the finding, the production of IL-17 upon phytohemagglutinin stimulation was assessed by multiplexed particle–based flow cytometry in patient 3. This showed minimal response (supplemental Figure 5).

Intact cytokine production in M394T-mutated patient with mycobacterial disease

Patient 3 with the *STAT3* M394T mutation developed disseminated mycobacterial disease in late adolescence. Because Mendelian susceptibility to mycobacterial disease generally involves defects in the IL-12/IFN-γ feedback loop,[23] the pathway was extensively tested but found normal. IFN-γ receptor–STAT1 signaling was intact, because STAT1 phosphorylation and upregulation of HLA-DR expression followed normal dose-response curves after in vitro stimulation with IFN-γ (data not shown). There was normal LPS-induced shedding of L-selectin (CD62L), suggesting normal Toll-like receptor signaling (data not shown).

Release of IL-12, TNF, and IFN-γ was normal after stimulation of PBMNCs with T-cell specific antigens. Notably, upon stimulation of PBMNCs with IL-12 plus LPS or IL-18, IFN-γ production was very low (supplemental Figure 5). These results suggested a defect in NK cell–mediated release of IFN-γ. However, flow cytometric assessment of intracellular IFN-γ production revealed normal production of IFN-γ on a per-cell basis (data not shown). Therefore, the reduced release of IFN-γ likely reflected the overall low frequency of NK cells among PBMNCs rather than a defect in NK cell function per se. The patient also tested negative for autoantibodies against various cytokines including IFN-γ, TNF, IL-12, IL-23, IFN-α, IFN-ω, IL-6, IL-17A, IL-17F, IL-22, and granulocyte macrophage–colony-stimulating factor (data not shown).

K392R-mutated patient developed T-cell LGL leukemia

Patient 2 with the STAT3 K392R mutation developed aberrant LGL proliferation, which was associated with megaloblastic anemia. In the detailed T-cell subset analysis, the phenotype of the abnormal cells was CD3$^+$TCR-γδ$^+$, and they accounted for 57% of all CD3$^+$ T cells (Figure 3D-F). However, the CD3$^+$TCR-γδ$^+$ population was not homogenous: 45% of the cells were CD8$^+$, whereas the rest had a TCR-γδ$^+$CD4$^-$CD8$^-$ immunophenotype (Figure 3D-F). The clonality of the LGL proliferation was confirmed by the positive result of a routine clinical TCR-γδ receptor polymerase chain reaction analysis. Because the LGL proliferation mainly consisted of CD4$^-$CD8$^-$ cells, we reviewed the patients' earlier CD4$^-$CD8$^-$ counts. All patients' proportions of CD3$^+$CD4$^-$CD8$^-$ T cells were above median (Table 2), but only in the K392R-mutated patient were they predominantly γδ T cells.

No cytogenetic alterations were found in the LGL subset in routine clinical investigations. To elucidate potential oncogenic single nucleotide variants driving the LGL expansion, the CD3$^+$ TCR γδ cells were exome sequenced in parallel with the germline DNA extracted from saliva sample. Four novel somatic mutations were called in the following genes: *LY9, RB1CC1, FOXP4 and ICOSLG* (Table 3). The variant allele frequency varied between 10% to 17%, suggesting that the mutations were located in a subpopulation of TCR-γδ$^+$ cells. No loss of heterozygosity for the germline *STAT3* K392R mutation was observed, and no genomic rearrangements were detected.

Discussion

In this study, we identified activating germline *STAT3* mutations K658N,[14] K392R,[14] and M394T in 3 patients with autoimmunity, hypogammaglobulinemia, lymphoproliferation, and mycobacterial disease. Autoimmunity and hypogammaglobulinemia were seen in all cases, and the displayed autoimmune phenomena are distinctly rare in children (desquamative interstitial pneumonitis, posterior uveitis). Lymphoproliferation (lymphadenopathy, splenomegaly, or pediatric T-cell LGL leukemia) was present in 2 cases. One patient developed disseminated mycobacterial disease in late adolescence. The patients presented with somewhat high proportions of CD3$^+$CD4$^-$CD8$^-$ T cells with decreased counts of dendritic, Treg, Th17, and NK cells as well as deficiency of switched memory B cells.

Heterozygous loss-of-function STAT3 mutations have been associated with autosomal dominant HIES, which is characterized by high serum IgE, eosinophilia, eczema, and immunodeficiency.[5,6] Our first patient developed eczema that differed from the typical hyper-IgE eczema clinically and histopathologically (data not shown). All patients were susceptible to respiratory infections, partly because of their hypogammaglobulinemia. No other features of HIES were

noted. The mutations in HIES localize to the DNA-binding and Src-like homolog 2 domains of STAT3, whereas the observed activating *STAT3* mutations scatter throughout the protein.[5,6,14] Mutations in the DNA-binding domain caused constitutive activation of STAT3, whereas the K658N mutation in the dimerization domain only conferred hypersensitivity to interleukins. The difference in action, however, does not correlate with the phenotype. It is possible that under physiologic conditions, hypersensitivity to low levels of interleukins is sufficient for persistent activation of STAT3 signaling.

Autoimmunity is commonly seen in patients with germline STAT mutations, sometimes with concomitant Treg deficiency.[2,3] (For comparison between IPEX-like syndromes caused by *STAT1, STAT3,* and *STAT5B* mutations, see supplemental Table 5). STAT3 promotes the activation and expansion of autoimmunity-associated Th17 cells, whereas STAT5 drives the immunosuppressive Treg fate. STAT3 and STAT5b bind to multiple sites of the IL-17 locus, with STAT3 binding promoting IL-17 transcription, and STAT5b binding conversely repressing IL-17 transcription.[24,25] Th17 deficiency is seen in loss-of-function *STAT3* mutations and HIES.[26,27] Curiously, our patients with activating STAT3 mutations also presented with a reduced number of Th17 cells and decreased IL-17 production.

A notable feature of the STAT3 hyperactivity patients was lymphoproliferation, which has not been described in other IPEX-like syndromes.[3] The somewhat elevated CD4$^-$CD8$^-$ T-cell counts observed in our patients may suggest a defect in lymphocyte apoptosis.[28] Notably, patient 2 (K392R) developed T-cell LGL leukemia at age 14. LGL leukemia is mainly diagnosed in the elderly and is often accompanied by autoimmune processes such as rheumatoid arthritis and autoimmune cytopenias. Somatic STAT3 gain-of-function mutations have been identified in 40% to 70% of T-cell LGL leukemia cases.[11-13] The occurrence of pediatric LGL leukemia in patient 1 and the presence of LGL-like cells in the BM of patient 2 suggest STAT3 is a central oncogene in LGL leukemia pathogenesis.

Patient 3 (M394T) presented only mild autoimmunity, but developed disseminated mycobacterial disease in late adolescence. In contrast to most known mycobacterial susceptibility syndromes,[23] IL-12–IFN-γ signaling was not impaired. Dendritic cell deficiencies cause mycobacterial disease,[29] and the observed lack of plasmacytoid dendritic cells may partly explain her condition. Why our IPEX-like patients has not developed mycobacterial infections is unknown. Because dendritic cell deficiency–associated mycobacterial disease onset is often late, the patients' young age might provide an explanation.

In conclusion, activating germline *STAT3* mutations lead to a broad range of immune disturbances, including multiorgan autoimmunity, lymphoproliferation, hypogammaglobulinemia, and delayed-onset mycobacterial disease. Emerging STAT3 inhibitors, some of which are in clinical trials, may benefit such patients. Our results provide insights into the role of STAT3 in the pathogenesis of autoimmune diseases and highlight the oncogenic nature of STAT3 in LGL leukemia development.

Authorship

Contribution: E.M.H. designed the study, coordinated the project, analyzed the data, and wrote the article; M.K. and H.L.M.R. contributed to writing the article and performed laboratory analysis; S.M., M.S., J.S., and J.K. designed and supervised the study, reviewed the data, and contributed to writing the article; Y.T.B., S.C., V.G., P.K., S.S., H.K., A.J.v.A., R.D., and A.H. designed and performed laboratory analysis; S.E., L.T., and R.K. designed and performed bioinformatics analysis; M.-L.K.-L. and P.E.K. reviewed the immunopathology; T.H.-K., T.O., M.S., K.P., R.U.-S., L.K., and K.H. provided clinical care for the patients; and all authors read and approved the final manuscript.

Conflict-of-interest disclosure: K.P. has received research funding and honoraria from Novartis and Bristol-Myers Squibb; S.M. has received honoraria from Novartis and Bristol-Myers Squibb; and M.S. has received honoraria from Octapharma and Sanquin. The remaining authors declare no competing financial interests.

Correspondence: Satu Mustjoki, Hematology Research Unit Helsinki, Helsinki University Central Hospital, Haartmaninkatu 8, PO Box 700, FIN-00290 Helsinki, Finland, e-mail: satu.mustjoki@helsinki.fi; Mikko Seppänen, Immunodeficiency Unit, Division of Infectious Diseases, Helsinki University Central Hospital, PO Box 348, FI-00290 Helsinki, Finland; e-mail: mikko.seppanen@hus.fi; and Janna Saarela, Institute for Molecular Medicine Finland, University of Helsinki, Tukholmankatu 8, PO Box 20, FIN-00290 Helsinki, Finland; e-mail: janna.saarela@helsinki.fi.

References

1. Bennett CL, Christie J, Ramsdell F, et al. The immune dysregulation, polyendocrinopathy, enteropathy, X-linked syndrome (IPEX) is caused by mutations of FOXP3. *Nat Genet.* 2001;27(1):20-21.

2. Uzel G, Sampaio EP, Lawrence MG, et al. Dominant gain-of-function STAT1 mutations in FOXP3 wild-type immune dysregulation-polyendocrinopathy-enteropathy-X-linked-like syndrome. *J Allergy Clin Immunol.* 2013;131(6):1611-1623.

3. Verbsky JW, Chatila TA. Immune dysregulation, polyendocrinopathy, enteropathy, X-linked (IPEX) and IPEX-related disorders: an evolving web of heritable autoimmune diseases. *Curr Opin Pediatr.* 2013;25(6):708-714.

4. Lohr NJ, Molleston JP, Strauss KA, et al. Human ITCH E3 ubiquitin ligase deficiency causes syndromic multisystem autoimmune disease. *Am J Hum Genet.* 2010;86(3):447-453.

5. Holland SM, DeLeo FR, Elloumi HZ, et al. STAT3 mutations in the hyper-IgE syndrome. *N Engl J Med.* 2007;357(16):1608-1619.

6. Minegishi Y, Saito M, Tsuchiya S, et al. Dominant-negative mutations in the DNA-binding domain of STAT3 cause hyper-IgE syndrome. *Nature.* 2007;448(7157):1058-1062.

7. Dupuis S, Jouanguy E, Al-Hajjar S, et al. Impaired response to interferon-alpha/beta and lethal viral disease in human STAT1 deficiency. *Nat Genet.* 2003;33(3):388-391.

8. Liu L, Okada S, Kong XF, et al. Gain-of-function human STAT1 mutations impair IL-17 immunity and underlie chronic mucocutaneous candidiasis. *J Exp Med.* 2011;208(8):1635-1648.

9. Knosp CA, Johnston JA. Regulation of CD4+ T-cell polarization by suppressor of cytokine signalling proteins. *Immunology.* 2012;135(2):101-111.

10. O'Shea JJ, Plenge R. JAK and STAT signaling molecules in immunoregulation and immune-mediated disease. *Immunity.* 2012;36(4):542-550.

11. Jerez A, Clemente MJ, Makishima H, et al. STAT3 mutations unify the pathogenesis of chronic lymphoproliferative disorders of NK cells and T-cell large granular lymphocyte leukemia. *Blood.* 2012;120(15):3048-3057.

12. Koskela HL, Eldfors S, Ellonen P, et al. Somatic STAT3 mutations in large granular lymphocytic leukemia. *N Engl J Med.* 2012;366(20): 1905-1913.

13. Fasan A, Kern W, Grossmann V, Haferlach C, Haferlach T, Schnittger S. STAT3 mutations are highly specific for large granular lymphocytic leukemia. *Leukemia.* 2013;27(7):1598-1600.

14. Flanagan SE, Haapaniemi E, Russell MA, et al. Activating germline mutations in STAT3 cause early-onset multi-organ autoimmune disease. *Nat Genet.* 2014;46(8):812-814.

15. Otonkoski T, Roivainen M, Vaarala O, et al. Neonatal type I diabetes associated with maternal echovirus 6 infection: a case report. *Diabetologia.* 2000;43(10):1235-1238.

16. Sulonen AM, Ellonen P, Almusa H, et al. Comparison of solution-based exome capture methods for next generation sequencing. *Genome Biol.* 2011;12(9):R94.

17. Ilander M, Kreutzman A, Rohon P, et al. Enlarged memory T-cell pool and enhanced Th1-type responses in chronic myeloid leukemia patients who have successfully discontinued IFN-α monotherapy. *PLoS ONE.* 2014;9(1):e87794.

18. Ruitenberg JJ, Boyce C, Hingorani R, Putnam A, Ghanekar SA. Rapid assessment of in vitro expanded human regulatory T cell function. *J Immunol Methods.* 2011;372(1-2):95-106.

19. Chiang SC, Theorell J, Entesarian M, et al. Comparison of primary human cytotoxic T-cell and natural killer cell responses reveal similar molecular requirements for lytic granule exocytosis but differences in cytokine production. *Blood.* 2013;121(8):1345-1356.

20. Schneider EM, Lorenz I, Müller-Rosenberger M, Steinbach G, Kron M, Janka-Schaub GE. Hemophagocytic lymphohistiocytosis is associated with deficiencies of cellular cytolysis but normal expression of transcripts relevant to killer-cell-induced apoptosis. *Blood.* 2002;100(8): 2891-2898.

21. Puel A, Döffinger R, Natividad A, et al. Autoantibodies against IL-17A, IL-17F, and IL-22 in patients with chronic mucocutaneous candidiasis and autoimmune polyendocrine syndrome type I. *J Exp Med.* 2010;207(2): 291-297.

22. Bromberg JF, Wrzeszczynska MH, Devgan G, et al. Stat3 as an oncogene. *Cell.* 1999;98(3): 295-303.

23. Cottle LE. Mendelian susceptibility to mycobacterial disease. *Clin Genet.* 2011;79(1): 17-22.

24. Yang XO, Panopoulos AD, Nurieva R, et al. STAT3 regulates cytokine-mediated generation of inflammatory helper T cells. *J Biol Chem.* 2007; 282(13):9358-9363.

25. Yang XP, Ghoreschi K, Steward-Tharp SM, et al. Opposing regulation of the locus encoding IL-17 through direct, reciprocal actions of STAT3 and STAT5. *Nat Immunol.* 2011;12(3):247-254.

26. Minegishi Y, Saito M, Nagasawa M, et al. Molecular explanation for the contradiction between systemic Th17 defect and localized bacterial infection in hyper-IgE syndrome. *J Exp Med.* 2009;206(6):1291-1301.

27. de Beaucoudrey L, Puel A, Filipe-Santos O, et al. Mutations in STAT3 and IL12RB1 impair the development of human IL-17-producing T cells. *J Exp Med.* 2008;205(7):1543-1550.

28. Magerus-Chatinet A, Stolzenberg MC, Loffredo MS, et al. FAS-L, IL-10, and double-negative CD4- CD8- TCR alpha/beta+ T cells are reliable markers of autoimmune lymphoproliferative syndrome (ALPS) associated with FAS loss of function. *Blood.* 2009;113(13):3027-3030.

29. Collin M, Bigley V, Haniffa M, Hambleton S. Human dendritic cell deficiency: the missing ID? *Nat Rev Immunol.* 2011;11(9):575-583.